Preprint

LS I +61°303 Radio Outburst Ephemeris

P. C. Gregory

Department of Physics and Astronomy,
University of British Columbia,
Vancouver, British Columbia, V6T 1Z1, Canada

gregory@physics.ubc.ca

ABSTRACT

The X and γ-ray binary and probable microquasar, LS I +61°303, is remarkable for its periodic radio outbursts every 26.5 days. It also exhibits a ~ 4.6 year periodic modulation of the phase and amplitude of these outbursts which may result from a resonant interaction between the neutron star and Be star primary. This paper provides a table of predicted outburst times and peak flux densities, along with their uncertainties, to aid in the planning and interpretation of future observations of this intriguing binary.

Subject headings: stars:emission-line — radio continuum:stars— Xrays:binaries— methods:data analysis

1. Introduction

The luminous, Be + neutron star X-ray binary, LS I +61°303 (V615 Cas, GT 0236+610) is particularly interesting because of its strong periodic radio outbursts every 26.5 days. The X-ray emission also exhibits a modulation at this period (e.g. Leahy 2001). In addition, LS I +61°303 is the probable counterpart to the γ-ray source, 2CG 135+01 (Gregory and Taylor 1978, Kniffen et al. 1997). The binary also exhibits a ~ 4.6 year periodic modulation of the phase and amplitude of these outbursts (e.g. Gregory 1999, Gregory et al. 1999). The shape of the peak flux density modulation is sinusoidal in appearance while the phase modulation exhibits a saw-tooth waveform. Recently, Gregory (2002) reported improved Bayesian estimates of both the orbital period P_1, and modulation period, P_2, based on the full Green Bank Interferometer (GBI) data set (Ray et al. 1997) and improved estimates

of the outburst times and peak flux densities. The new estimates are $P_1 = 26.4960 \pm .0028$ days and $P_2 = 1667 \pm 8$ days.

Massi et al. (2001) have found evidence for a jet like structure in recent Merlin and EVN observations of the source and suggest that the intrinsic velocity may be as large as 0.4 c. It is tempting to suppose that the 1667 day modulation in the outburst peak flux density results from variations in Doppler beaming arising from jet precession. However, such a mechanism does not account for the observed saw tooth shaped modulation of the outburst orbital phase with the same period (Gregory 2002).

Gregory (2002) provided evidence that indicates that the orbit of the neutron star is embedded in the Be star equatorial disk. Zamanov and Martí (2000) have also recently demonstrated a modulation on the same time scale, in the EW(H_α) and $\Delta V_{\rm peak}$, the H_α equivalent width and double peak velocity separation, respectively. This latter results strongly suggests that the modulation in the radio emission is related to changes in the Be star equatorial disk properties. Gregory and Neish (2002) have shown how to use the variable radio emission to investigate the temporal properties of the Be star equatorial mass loss. Their analysis indicates that the ~ 4.6 year modulation in radio properties results from periodic outward moving density enhancements in the equatorial disk. They also propose that each new ejection phase may be triggered by the interaction of a short lived relativistic wind (ejector phase) from the neutron star, with the rapidly rotating Be star primary.

Many questions remain and further testing of these models are required, especially at X-ray and γ-ray wavelengths. We also need an improved determination of the orbit of the system.

2. Ephemeris

Now that the GBI monitoring program has ended, there is clearly a need for an ephemeris to predict the known periodic properties of the radio outbursts for comparison with other observations. The ephemeris presented here is based on the latest analysis (Gregory, 2002) of all the radio data taken up to and including Julian Day (JD) 2,451,823.8, a time span of 23.2 years. Only data within the frequency range 5 to 10.5 GHz was used in the analysis.

In the absence of precise knowledge of periastron, we have by convention defined the zero of orbital phase as t_r (JD $= 2,443,366.775$), the date of the first radio detection of the star. This is often referred to in the literature as radio phase. Orbital phase, θ_1, and

modulation P_2 phase, θ_2, are given by:

$$\theta_1 = \frac{(\mathrm{JD} - t_r)}{P_1} - \text{Integer part}\left[\frac{(\mathrm{JD} - t_r)}{P_1}\right], \tag{1}$$

where $P_1 = 26.4960$ days.

$$\theta_2 = \frac{(\mathrm{JD} - t_r)}{P_2} - \text{Integer part}\left[\frac{(\mathrm{JD} - t_r)}{P_2}\right], \tag{2}$$

where $P_2 = 1667$ days. Thus θ_1 is a phase which varies between 0 and 1, and similarly for θ_2. A table of the Bayesian mean outburst timing residuals and mean outburst peak flux densities, versus P_2 phase, is given in Table 1 along with their one σ uncertainties. Figure 1 is a plot of these quantities. Panel (a) shows the mean timing residual light-curve, $\pm 1\sigma$. Panel (c) shows the individual outburst timing residuals, computed for the most probable outburst period of $P_1 = 26.496$ days and the most probable modulation period of $P_2 = 1667$ days, overlaid on the timing residual light-curve of panel (a). Panel (b) shows a plot of the mean outburst peak flux density light-curve, $\pm 1\sigma$. Panel (d) shows the individual outburst peak flux densities overlaid on the light-curve of panel (b).

As previously mentioned, the P_1 and P_2 phase data derived by Gregory (2002) is relative to JD 2,443,366.775, the date of the first radio observation. For the purpose of forecasting the times of future outbursts it is desirable to pick a later reference epoch to minimize the prediction errors due to uncertainties in P_1 and P_2. Since the timing residuals are relative to a much later epoch, $t_0 =$ JD 2,449,849, it is convenient to use t_0 as the new reference epoch.

We have used the above information to compute a table of predicted mean outburst times and mean peak flux densities, for a time interval of approximately 30 years post t_0, together with their estimated errors. Successive outbursts are indexed according to the outburst number, k. This was accomplished by a Monte Carlo calculation involving randomly sampling Gaussian approximations to the probability density functions for P_1 and P_2 and the timing residuals. For each value of k, 1000 predictions were made using this Monte Carlo approach. The individual predictions are indexed according to the integer variable, i. The final prediction for the k^{th} outbursts, and its uncertainty, were obtained from the mean and standard deviation of the 1000 individual predictions. The steps involved in the calculation are as follows:

1. Use a Gaussian random number generator, with mean = 26.496 days and standard deviation = 0.0028 days, to select a value for P_{1i}.

2. For each value of the outburst number, k, compute the nominal outburst time, t_{ni}, according to

$$t_{ni} = t_0 + k \times P_{1i} \tag{3}$$

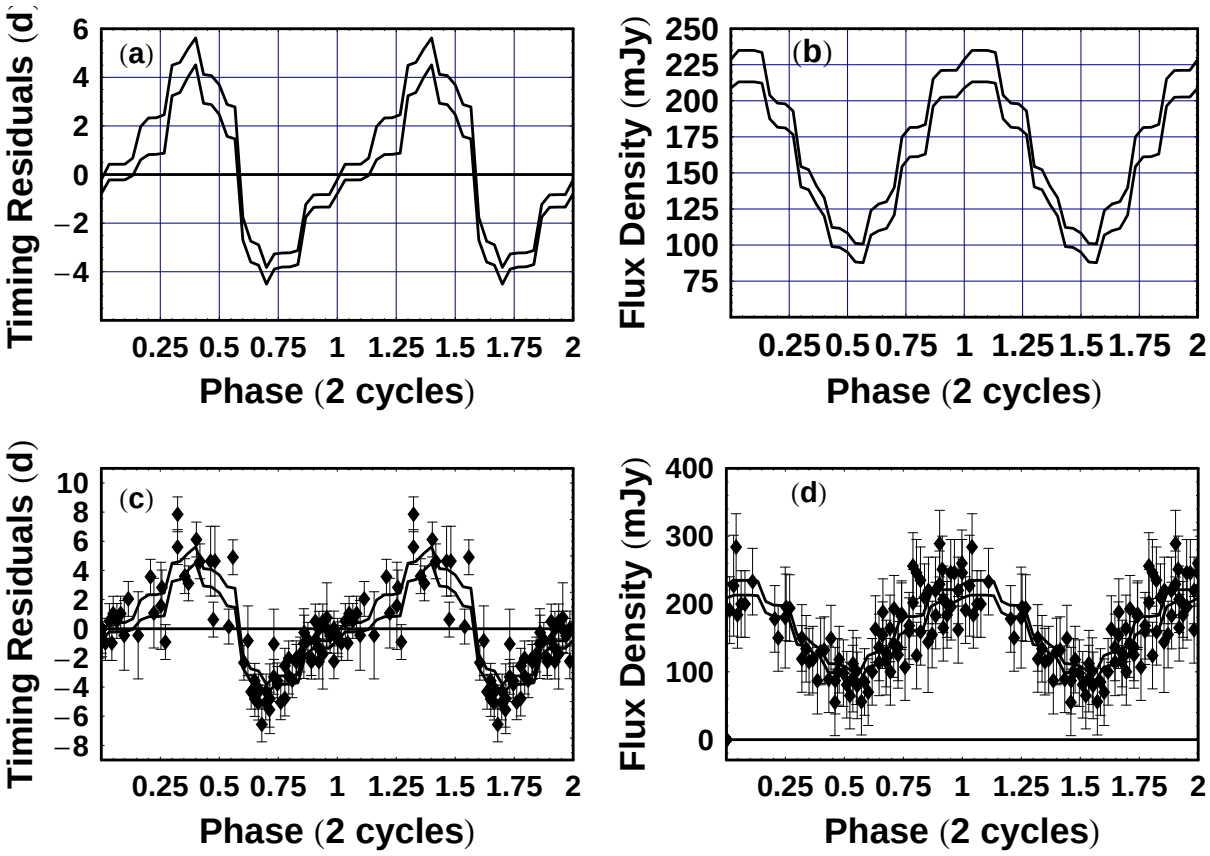

Fig. 1.— Panel (a) shows the Bayesian mean timing residual light-curve, $\pm 1\sigma$. Panel (c) shows the individual outburst timing residuals, computed for the most probable $P_1 = 26.496$ days and the most probable $P_2 = 1667$ days, overlaid on the timing residual light-curve of panel (a). Panel (b) shows the Bayesian mean outburst peak flux density light-curve, $\pm 1\sigma$. Panel (d) shows the individual outburst peak flux densities overlaid on the light-curve of panel (b).

where t_0 is the timing residual reference outburst, JD = 2,449,849.0.

3. Use a Gaussian random number generator, with mean = 1667 days and standard deviation = 8 days, to select a value for P_{2i}.

4. Compute an estimate of the P_2 phase, θ_{2i}, of the k^{th} outburst, according to

$$\theta_{2i} = \frac{(t_{ni} - t_0)}{P_2} - \text{Integer part}\left[\frac{(t_{ni} - t_0)}{P_2}\right], \tag{4}$$

5. The result from step (4), θ_{2i}, is a phase relative to epoch t_0. We next want to obtain an estimate of the outburst timing residual, τ_i, and its uncertainty, $\tau_{\sigma i}$, corresponding to θ_{2i}. However, these quantities, as given in Table 1 and Figure 1, are a function of a phase referred to t_r. We need to convert the θ_{2i} value to a phase, θ_{ri}, relative to t_r before interpolating Table 1 for values of τ_i, $\tau_{\sigma i}$, S_i, and $S_{\sigma i}$. Let θ_0 be the P_2 phase of reference outburst t_0 relative to t_r. This is given by:

$$\theta_0 = \frac{(t_0 - t_r)}{P_2} - \text{Integer part}\left[\frac{(t_0 - t_r)}{P_2}\right] = 0.8886 \tag{5}$$

Then θ_{ri} is given by the following algorithm:

$$\theta_x = \theta_{2i} + \theta_0 \tag{6}$$

$$\text{If } \theta_x \leq 1, \text{ then } \theta_{ri} = \theta_x, \text{ otherwise } \theta_{ri} = \theta_x - 1. \tag{7}$$

6. Compute a first estimate of the outburst timing residual, τ_1, and timing residual uncertainty, $\tau_{\sigma 1}$, by interpolating the entries in Table 1 for a phase = θ_{ri}.

7. Use a Gaussian random number generator, with mean = τ_1 and standard deviation = $\tau_{\sigma 1}$, to select a value for τ_i.

8. Repeat steps 3 to 5 one more time, to refine the estimate of θ_{ri}, replacing t_{ni} by $t_{ni} + \tau_i$.

9. Interpolate Table 1, using the latest θ_{ri}, to obtain second estimates: $\tau_2, \tau_{\sigma 2}, S_2$, and $S_{\sigma 2}$.

10. Use a Gaussian random number generator, with mean = τ_2 days and standard deviation = $\tau_{\sigma 2}$ days, to select a value for τ_i. Use a Gaussian random number generator, with mean = S_2 and standard deviation = $S_{\sigma 2}$, to select a value for S_i.

11. Finally we arrive at one prediction for the k^{th} outburst time, $t_i = t_{ni} + \tau_i$ and its associated flux density S_i.

12. Repeat steps 1 to 11, until we have 1000 estimates of t_i and S_i.

13. The final prediction for the k^{th} outbursts and its uncertainty, are obtained from the mean and standard deviation of the 1000 individual predictions.

The predictions for a 30 year period, post JD = 2,449,849, are given in Tables 2 to 5. The columns are: 1) the JD of the predicted mean outburst peak, 2) the uncertainty in predicted time, 3) the predicted mean peak flux density, and 4) the uncertainty in the peak flux density. Figure 2 shows the uncertainty in the predicted mean outburst time and mean peak flux density (S), versus outburst number.

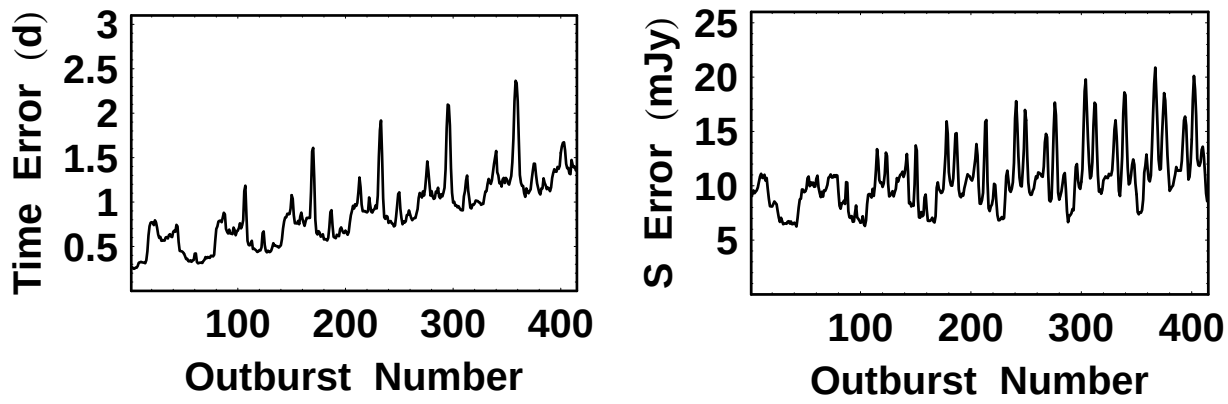

Fig. 2.— The uncertainty in the predicted outburst time and peak flux density (S), versus outburst number. Outburst zero corresponds to JD 2,449,849.

The predicted quantities were compared to the actual outburst times and peak flux densities measured in a cross correlation analysis (Gregory 2002) of the 41 outbursts recorded by the GBI data post JD 2,449,849. The standard deviation of the residuals was 1.45 days and 33 mJy, respectively. The residuals are composed of three quadrature components: a) the uncertainty in the predicted mean values, b) the uncertainty in the measured quantities for the individual outbursts, and c) variability in the outbursts not accounted for by the two period model assumed in the analysis. These 41 outburst span an interval of 68 P_1 periods post t_0. Examination of Figure 2 indicates that only a small part of the residuals are accounted for by the uncertainties in the predicted quantities. A Bayesian analysis of the effective measurement noise indicates that other potentially interesting processes, like smaller amplitude and shorter duration variability, remain to be characterized.

The Green Bank Interferometer is a facility of the National Science Foundation operated by the National Radio Astronomy Observatory. From 1978-1996, it was operated in support

of USNO and NRL geodetic and astronomy programs; after 1996 in support of NASA High Energy Astrophysics programs. The NRAO is operated by Associated Universities, Inc., under contract with the National Science Foundation. This research was supported in part by grants from the Canadian Natural Sciences and Engineering Research Council at the University of British Columbia.

REFERENCES

Gregory, P. C. and Taylor, A. R. 1978, Nature, 272, 704

Gregory, P. C. 1999, ApJ, 520, 361

Gregory, P. C., Peracaula, M. and Taylor, A.R. 1999, ApJ, 520, 376

Gregory, P. C. 2002, ApJ, 575, 427

Gregory, P. C. and Neish C. 2002, ApJ, 580, 1133

Kniffen, D. A. et al. 1997, ApJ, 486, 126

Waters, L. B. F. M. 1987, ApJ, 182, 80

Leahy, D. A. 2001, A&A, 380, 516

Massi, M., Ribó, M., Paredes, J.M., Peracaula, M., & Estalella, R. 2001, A&A, 376, 217

Massi, M., Ribó, M., Paredes, J.M., Peracaula, M., Martí, J. & Garrington, S. T. 2003, in "New Views of Microquasars", Proceedings of the 4th Microquasar Workshop, eds. Ph Durouchoux,Y. Fuchs and J. Rodriguez, published by the Center for Space Physics: Kolkata

Ray, P. S., Foster, R.S., Waltman, E. B. et al. 1997, ApJ, 491, 381

Zamanov, R. K., and Martí, J. 2000, A&A, 358, L55

P2 Phase	t Residual days	Error days	S mJy	Error mJy
0.	-0.5	0.28	219	10
0.03	0.1	0.32	224	11
0.06	0.1	0.32	224	11
0.1	0.1	0.32	224	11
0.13	0.32	0.35	223	11
0.16	1.28	0.68	196	8
0.2	1.57	0.75	190	8
0.23	1.58	0.75	190	8
0.26	1.67	0.79	185	8
0.3	3.87	0.62	147	7
0.33	3.99	0.61	145	7
0.36	4.58	0.57	135	6
0.4	5.06	0.55	126	6
0.43	3.52	0.59	106	7
0.46	3.47	0.59	105	7
0.5	3.08	0.61	102	7
0.53	2.22	0.65	95	6
0.56	2.12	0.65	94	6
0.6	-2.22	0.46	115	8
0.63	-3.17	0.42	119	9
0.66	-3.31	0.41	121	9
0.7	-4.16	0.34	130	9
0.73	-3.57	0.31	165	10
0.76	-3.51	0.28	171	10
0.8	-3.5	0.28	171	10
0.83	-3.41	0.28	173	10
0.86	-1.49	0.26	206	9
0.9	-1.09	0.25	212	9
0.93	-1.08	0.25	212	9
0.96	-1.08	0.25	212	9
1.	-0.5	0.28	219	10

Table 1: Tabular values of Bayesian mean timing residual light-curve and one σ uncertainty, and the mean outburst peak flux density and one σ uncertainty, versus P_2 modulation phase. The P_2 phase zero is JD 2,443,366.775.

Time JD	Error days	S mJy	Error mJy	Time JD	Error days	S mJy	Error mJy
2449874.4	0.26	212	9	2451249.6	0.34	160	11
2449900.9	0.25	212	9	2451276.2	0.33	168	10
2449927.3	0.24	212	9	2451302.7	0.33	171	10
2449953.8	0.24	212	9	2451329.2	0.32	172	10
2449980.3	0.25	212	10	2451355.7	0.33	172	10
2450007.0	0.26	214	10	2451382.2	0.32	171	10
2450033.9	0.29	218	10	2451408.7	0.34	171	10
2450060.8	0.3	222	11	2451435.7	0.43	179	11
2450087.5	0.32	224	11	2451463.2	0.42	196	11
2450114.1	0.32	224	11	2451490.4	0.33	208	10
2450140.5	0.33	225	11	2451517.1	0.29	211	9
2450167.0	0.31	225	10	2451543.6	0.31	212	9
2450193.5	0.31	224	11	2451570.1	0.3	212	10
2450220.0	0.31	225	11	2451596.6	0.32	212	9
2450246.6	0.33	224	11	2451623.1	0.32	211	9
2450273.5	0.45	215	10	2451649.6	0.31	212	9
2450300.5	0.61	201	9	2451676.3	0.34	214	9
2450327.3	0.7	193	8	2451703.2	0.39	219	10
2450353.9	0.77	191	8	2451730.1	0.39	222	11
2450380.5	0.76	190	9	2451756.8	0.39	223	10
2450406.9	0.76	190	8	2451783.3	0.39	224	11
2450433.4	0.74	190	8	2451809.8	0.37	224	11
2450459.9	0.79	188	8	2451836.2	0.38	224	11
2450486.7	0.79	180	8	2451862.7	0.37	225	11
2450514.4	0.7	161	8	2451889.3	0.39	226	11
2450541.8	0.62	146	7	2451915.9	0.42	224	11
2450568.4	0.6	145	7	2451942.8	0.53	214	11
2450594.9	0.62	144	7	2451969.7	0.69	201	10
2450621.6	0.6	140	7	2451996.6	0.78	192	8
2450648.4	0.58	134	6	2452023.2	0.8	190	8
2450675.3	0.56	131	6	2452049.7	0.78	189	8
2450701.8	0.55	126	6	2452076.3	0.79	190	8
2450727.7	0.58	116	7	2452102.6	0.79	190	8
2450753.4	0.59	107	7	2452129.1	0.8	188	8
2450779.7	0.6	104	7	2452156.2	0.91	178	10
2450806.3	0.62	105	7	2452183.8	0.87	160	10
2450832.7	0.6	104	7	2452211.0	0.67	147	7
2450859.0	0.6	102	7	2452237.6	0.67	145	7
2450885.1	0.63	100	7	2452264.1	0.66	144	7
2450911.2	0.66	95	6	2452290.9	0.65	139	7
2450937.6	0.67	94	6	2452317.7	0.65	134	7
2450964.1	0.67	93	7	2452344.5	0.62	131	6
2450989.6	0.75	98	7	2452371.0	0.64	125	8
2451014.2	0.74	108	8	2452396.9	0.68	115	8
2451038.9	0.54	115	9	2452422.7	0.7	107	7
2451064.8	0.46	118	9	2452449.0	0.67	105	7
2451091.1	0.46	119	9	2452475.5	0.68	105	7
2451117.5	0.45	119	9	2452501.9	0.69	103	7
2451143.9	0.44	120	9	2452528.1	0.7	102	7
2451170.1	0.44	123	9	2452554.3	0.69	99	7
2451196.2	0.38	129	10	2452580.5	0.71	95	7
2451222.7	0.36	143	11	2452606.9	0.73	93	7

Table 2: Predicted outburst times and flux densities and estimated one σ uncertainties.

JD	days	mJy	mJy	JD	days	mJy	mJy
2452633.3	0.77	94	7	2454013.7	0.73	130	8
2452658.6	1.12	99	8	2454040.1	0.8	123	9
2452683.3	1.25	108	9	2454066.0	0.88	114	10
2452708.3	0.83	115	9	2454092.0	0.83	107	8
2452734.1	0.58	118	9	2454118.3	0.74	105	7
2452760.3	0.52	120	9	2454144.8	0.71	104	7
2452786.8	0.52	120	9	2454171.1	0.75	104	7
2452813.1	0.5	121	9	2454197.4	0.8	102	7
2452839.2	0.56	124	10	2454223.5	0.85	99	7
2452865.4	0.47	131	11	2454249.8	0.82	96	7
2452892.0	0.5	145	14	2454276.1	0.86	94	7
2452918.8	0.47	160	12	2454302.3	1.09	95	8
2452945.4	0.44	169	10	2454327.6	1.52	101	9
2452972.0	0.44	170	10	2454352.4	1.65	109	11
2452998.5	0.44	171	10	2454377.6	1.14	115	10
2453024.9	0.44	171	10	2454403.4	0.75	118	9
2453051.4	0.45	171	10	2454429.6	0.66	120	9
2453078.0	0.48	172	11	2454456.0	0.66	120	9
2453105.1	0.67	182	13	2454482.3	0.66	122	10
2453132.4	0.65	197	14	2454508.5	0.64	126	10
2453159.6	0.53	208	10	2454534.8	0.63	133	13
2453186.3	0.45	211	9	2454561.3	0.65	147	16
2453212.9	0.44	212	9	2454588.1	0.6	160	15
2453239.4	0.43	212	9	2454614.7	0.6	168	11
2453265.9	0.43	212	9	2454641.2	0.56	170	10
2453292.3	0.44	212	9	2454667.7	0.58	171	10
2453318.9	0.46	213	10	2454694.2	0.57	172	10
2453345.7	0.48	215	10	2454720.7	0.61	172	10
2453372.5	0.54	219	10	2454747.4	0.7	175	11
2453399.3	0.53	222	11	2454774.4	0.88	184	16
2453426.0	0.51	224	11	2454801.7	0.88	197	14
2453452.5	0.47	224	11	2454828.8	0.71	206	11
2453479.0	0.51	223	11	2454855.5	0.6	211	10
2453505.5	0.5	223	11	2454882.1	0.59	212	9
2453532.0	0.48	225	11	2454908.6	0.58	212	9
2453558.6	0.51	224	11	2454935.1	0.61	212	9
2453585.2	0.57	222	12	2454961.6	0.6	212	9
2453612.1	0.71	212	13	2454988.2	0.64	213	10
2453639.0	0.77	201	11	2455014.9	0.68	216	10
2453665.8	0.89	193	9	2455041.7	0.7	219	10
2453692.4	0.85	191	8	2455068.5	0.66	222	11
2453718.9	0.89	190	8	2455095.2	0.63	224	11
2453745.4	0.83	189	8	2455121.7	0.64	224	11
2453771.9	0.9	189	8	2455148.3	0.64	224	11
2453798.5	0.95	186	9	2455174.7	0.63	225	11
2453825.6	1.04	176	13	2455201.2	0.66	224	11
2453853.0	1.03	159	13	2455227.8	0.64	223	11
2453880.2	0.83	147	9	2455254.5	0.75	219	13
2453906.9	0.76	145	7	2455281.3	0.88	211	14
2453933.5	0.78	143	7	2455308.3	0.92	201	13
2453960.2	0.74	139	7	2455335.0	0.98	194	10
2453987.0	0.82	134	7	2455361.6	0.96	190	9
2454013.7	0.73	130	8	2455388.1	0.98	190	8

Table 3: Predicted outburst times and flux densities and estimated one σ uncertainties.

JD	days	mJy	mJy	JD	days	mJy	mJy
2455414.7	0.95	189	8	2456791.0	0.79	224	11
2455441.2	0.97	189	9	2456817.5	0.8	224	11
2455467.8	1.12	183	12	2456844.0	0.83	224	10
2455495.0	1.26	172	16	2456870.6	0.8	224	11
2455522.3	1.2	159	16	2456897.1	0.87	222	12
2455549.4	0.97	149	12	2456923.8	0.93	218	14
2455576.1	0.93	145	8	2456950.7	1.02	210	15
2455602.8	0.9	143	8	2456977.5	1.04	201	14
2455629.5	0.94	138	8	2457004.3	1.09	195	12
2455656.3	0.89	134	8	2457030.9	1.09	191	9
2455682.9	0.86	129	9	2457057.4	1.03	190	8
2455709.2	0.93	122	11	2457083.9	1.05	189	9
2455735.3	0.98	115	11	2457110.5	1.12	186	11
2455761.3	0.94	109	9	2457137.3	1.28	182	14
2455787.5	0.9	105	7	2457164.3	1.36	170	18
2455813.9	0.89	104	7	2457191.5	1.38	159	16
2455840.3	0.91	103	7	2457218.5	1.26	150	13
2455866.6	0.96	102	7	2457245.4	1.04	145	9
2455892.8	0.95	98	7	2457272.1	1.02	141	9
2455919.0	0.96	96	7	2457298.7	1.04	137	9
2455945.2	1.04	95	7	2457325.5	1.06	133	10
2455971.2	1.42	97	9	2457352.0	1.06	128	10
2455996.6	1.94	102	11	2457378.3	1.11	122	11
2456021.6	1.93	109	11	2457404.5	1.09	114	12
2456046.8	1.52	114	10	2457430.7	1.09	109	10
2456072.7	1.05	118	9	2457456.8	1.06	106	8
2456098.9	0.85	119	9	2457483.2	1.03	104	7
2456125.2	0.79	121	9	2457509.5	1.03	103	7
2456151.5	0.82	123	10	2457535.8	1.1	100	7
2456177.7	0.81	127	13	2457561.9	1.12	99	8
2456204.1	0.82	136	17	2457588.2	1.17	96	7
2456230.6	0.75	148	18	2457614.3	1.37	96	8
2456257.3	0.78	158	16	2457640.1	1.9	98	10
2456283.9	0.77	167	13	2457665.5	2.11	103	12
2456310.5	0.71	170	11	2457690.9	2.13	109	12
2456336.9	0.74	171	10	2457716.3	1.71	113	11
2456363.4	0.74	171	11	2457742.1	1.37	117	10
2456390.0	0.8	173	11	2457768.1	1.07	119	10
2456416.8	0.94	178	14	2457794.4	1.04	121	10
2456443.8	1.13	187	16	2457820.8	0.97	123	11
2456471.0	1.08	198	16	2457847.0	0.96	129	15
2456498.0	0.88	205	13	2457873.4	0.93	138	19
2456524.8	0.82	210	10	2457899.9	0.96	149	19
2456551.3	0.75	212	9	2457926.5	0.95	159	17
2456577.9	0.75	211	9	2457953.1	0.91	166	15
2456604.3	0.76	212	9	2457979.6	0.93	169	12
2456630.9	0.77	213	10	2458006.2	0.89	171	11
2456657.5	0.81	214	10	2458032.7	0.91	172	11
2456684.2	0.87	216	10	2458059.4	0.98	175	12
2456711.0	0.91	219	11	2458086.2	1.23	178	16
2456737.8	0.87	222	11	2458113.1	1.3	188	18
2456764.4	0.81	224	11	2458140.2	1.28	197	17
2456791.0	0.79	224	11	2458167.2	1.15	204	14

Table 4: Predicted outburst times and flux densities and estimated one σ uncertainties.

Time JD	Error days	S mJy	Error mJy	Time JD	Error days	S mJy	Error mJy
2458193.9	1.	209	12	2459490.0	1.14	125	14
2458220.5	0.91	211	10	2459516.3	1.14	132	17
2458247.1	0.92	212	9	2459542.7	1.1	139	20
2458273.6	0.89	212	10	2459569.2	1.13	149	20
2458300.1	0.95	213	9	2459595.7	1.09	158	19
2458326.8	1.01	214	10	2459622.4	1.07	164	15
2458353.5	1.03	216	11	2459648.9	1.06	169	13
2458380.3	1.06	219	11	2459675.5	1.11	171	11
2458407.0	1.01	221	11	2459702.1	1.12	172	12
2458433.7	1.01	223	11	2459728.7	1.28	176	14
2458460.3	1.	224	11	2459755.6	1.38	181	17
2458486.7	0.97	224	11	2459782.5	1.47	189	18
2458513.2	0.95	224	11	2459809.5	1.42	196	18
2458539.8	1.	222	12	2459836.4	1.35	204	15
2458566.4	1.07	222	13	2459863.1	1.25	209	12
2458593.2	1.14	216	15	2459889.7	1.16	211	10
2458619.9	1.18	209	16	2459916.3	1.14	211	10
2458646.7	1.22	203	15	2459942.8	1.13	212	10
2458673.4	1.19	195	12	2459969.4	1.17	213	10
2458700.0	1.24	192	9	2459996.1	1.15	215	10
2458726.7	1.2	190	10	2460022.7	1.19	217	11
2458753.3	1.27	189	10	2460049.6	1.24	219	11
2458779.9	1.33	185	13	2460076.2	1.17	221	11
2458806.7	1.4	179	17	2460102.8	1.13	223	11
2458833.7	1.64	170	19	2460129.4	1.15	224	11
2458860.8	1.5	160	18	2460156.0	1.14	223	11
2458887.6	1.36	152	15	2460182.5	1.14	223	11
2458914.6	1.33	145	12	2460209.1	1.19	222	12
2458941.3	1.19	141	10	2460235.8	1.23	219	13
2458968.0	1.18	137	10	2460262.5	1.32	215	15
2458994.7	1.2	132	11	2460289.2	1.33	207	17
2459021.1	1.2	127	12	2460316.0	1.36	202	15
2459047.5	1.29	120	13	2460342.7	1.39	197	13
2459073.6	1.29	114	12	2460369.3	1.31	192	11
2459099.9	1.29	110	10	2460395.9	1.39	190	10
2459126.1	1.21	107	9	2460422.6	1.45	187	12
2459152.5	1.2	104	8	2460449.2	1.49	183	15
2459178.7	1.18	103	7	2460476.0	1.64	176	19
2459205.0	1.24	101	8	2460503.0	1.73	169	20
2459231.2	1.28	98	8	2460530.1	1.73	159	18
2459257.5	1.41	97	8	2460557.0	1.56	151	16
2459283.4	1.73	97	9	2460583.9	1.51	146	13
2459309.0	2.11	99	10	2460610.6	1.43	141	12
2459334.7	2.32	104	12	2460637.2	1.41	136	11
2459360.0	2.31	109	13	2460663.9	1.36	131	12
2459385.6	2.07	113	12	2460690.3	1.38	126	13
2459411.4	1.65	117	11	2460716.6	1.41	120	14
2459437.4	1.33	119	10	2460742.9	1.48	115	13
2459463.7	1.21	122	10	2460769.2	1.44	110	11
2459490.0	1.14	125	14	2460795.3	1.38	107	9

Table 5: Predicted outburst times and flux densities and estimated one σ uncertainties.